Supplementary material for "Simultaneous real and momentum space electron diffraction from a fullerene molecule"

R. Aiswarya,[1] Rasheed Shaik,[2] Jobin Jose,[1,*] Hari R. Varma,[2] and Himadri S. Chakraborty[3,†]

[1] *Department of Physics, Indian Institute of Technology Patna, Bihar 801103, India*
[2] *School of Physical Sciences, Indian Institute of Technology Mandi, Kamand, H.P. 175075, India*
[3] *Department of Natural Sciences, D.L. Hubbard Center for Innovation, Northwest Missouri State University, Maryville, Missouri 64468, USA*

C_{60} MODELING

We use the atomic units (a.u.) unless specified otherwise. The C_{60} environment is simulated using two distinct model potentials: one using the density functional theory (DFT) within the local density approximation (LDA) [1, 2] and the other employing the static annular square well (ASW) model [3]. In the DFT description, the positively charged ionic core created by sixty C_4^+ ions is approximated by an attractive jellium potential $V_{\rm Jel}$. A constant pseudo potential [4] is added by imposing the charge neutrality of the system to improve the quantitative accuracy [2]. This produced a close agreement with the first ionization threshold of 7.54 eV for C_{60} known from the experiment [5] and the C_{60} shell thickness Δ to be 2.41 a.u. around the known molecular radius of 6.70 a.u. The ground-state electron density $\rho(r)$ of C_{60} is obtained by solving the Kohn-Sham equations for a system of 240 electrons (four valence electrons from each of sixty carbon atoms). For the e-C_{60} interaction, the radial DFT-LDA potential can be written as:

$$V_{\rm DFT}(r) = V_{\rm Jel}(r) + \int \frac{\rho(r')}{r-r'}dr' + V_{\rm XC}(\rho(r)), \qquad (1)$$

where the second and the third term on the right hand side, respectively, denote the direct and exchange-correlation interactions. The exchange-correlation potential used in the present study is [1]:

$$V_{\rm XC}(\rho(r)) = -\left(\frac{3\rho(r)}{\pi}\right)^{1/3} - 0.0333\ln\left[1+11.4\left(\frac{4\pi\rho(r)}{3}\right)^{1/3}\right]. \qquad (2)$$

In Eq. (2), the first and the second term embody the exchange and the correlation effects, respectively. Hartree-Fock formalism within LDA was used to derive the exchange potential form [1].

The ASW potential is defined as [3]:

$$V_{\rm ASW} = \begin{cases} -U, & r_i \le r \le r_o, \\ 0, & \text{otherwise} \end{cases}, \qquad (3)$$

where the inner radius $r_i = r_c - \frac{\Delta}{2} = 5.26$ a.u. and the outer radius $r_o = r_c + \frac{\Delta}{2} = 8.17$ a.u. The mean radius r_c and thickness Δ of C_{60} cage are taken to be 6.70 a.u. and 2.91 a.u. This value of Δ matches the diameter of a carbon atom. The well depth $U = 0.26$ a.u. is chosen in such a way that it simulates the correct C_{60} electron affinity, 2.65 eV known from experiment [6].

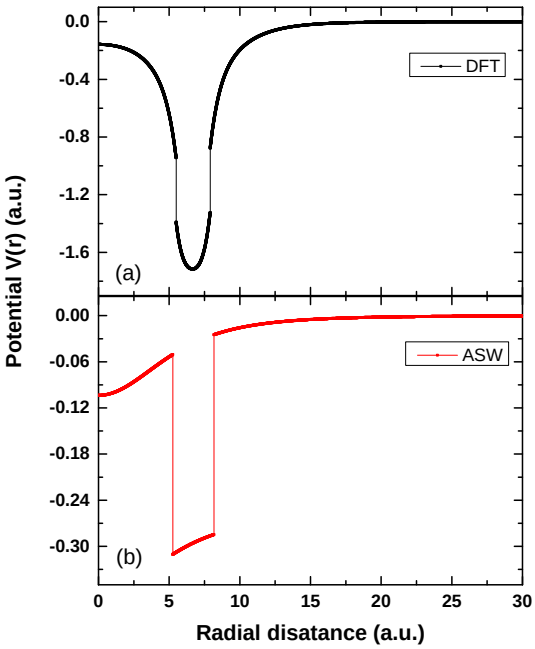

FIG. 1. (Color online) DFT (a) and ASW (b) e-C_{60} interaction potentials.

The polarization effect must be taken into consideration for a meaningful assessment of projectile-target interaction. This effect is approximated by the long-range static polarization potential of the form [7]:

$$V_{\rm Pol} = \frac{-\alpha}{2\left(r^2+b^2\right)^2}, \qquad (4)$$

where $\alpha = 850$ a.u. is the static dipole polarizability and $b = 8$ a.u. is the cut-off parameter of C_{60}. This polarization potential is added to both the DFT [Eq. (1)] and ASW [Eq. (3)] potentials in order to obtain the final e-C_{60} interaction potentials:

$$V_{C_{60}} = V_{\rm DFT/ASW} + V_{\rm Pol}. \qquad (5)$$

A comparison of these interaction potentials is presented in Fig. 1

PARTIAL WAVE ANALYSIS

The scattering state wave function in e-C_{60} collision is the solution of the radial Schrödinger equation [8, 9]:

$$\left\{ \frac{-\hbar^2}{2m}\frac{d^2}{dr^2} + \left[V_{C_{60}} + \frac{\hbar^2 \ell(\ell+1)}{2mr^2} \right] \right\} u_\ell(r) = E u_\ell(r). \tag{6}$$

Here $u_\ell(r)$ is the scaled radial wave function for a given angular momentum quantum number ℓ, and $V_{C_{60}}$ is the model potentials (DFT/ASW) as defined in Eq. (5). The solution of Eq. (6) is obtained using Numerov's method [9] with a radial grid size of 0.001 a.u. The scattering phase shift (δ_ℓ) of the ℓ-th partial wave is evaluated using the asymptotic wave function form given by [8]:

$$u_\ell(r > r_{\max}) \propto kr[j_\ell(kr)\cos\delta_\ell - n_\ell(kr)\sin\delta_\ell]. \tag{7}$$

For a given incident energy E, the incident momentum (or the wave vector) $k = \sqrt{2E}$ (in a.u.). Also, j_ℓ and n_ℓ are Bessel functions of the first and second kind, respectively. $r_{\max}$ represents the practical radial infinity, which in the present study is taken to be 28 a.u. Beyond this distance, the scattering center has no interaction effect on the scattered particle. Let r_1 and r_2 be the two asymptotic radial points beyond the interaction region ($r > r_{\max}$), using which phase shift (δ_ℓ) can be computed [8] by,

$$\tan(\delta_\ell(k)) = \frac{\xi j_\ell(kr_1) - j_\ell(kr_2)}{\xi n_\ell(kr_1) - n_\ell(kr_2)}, \tag{8}$$

where

$$\xi = \frac{r_1 u_\ell(r_2)}{r_2 u_\ell(r_1)}. \tag{9}$$

The numerical values of the Bessel functions (j_ℓ and n_ℓ) are obtained by using standardized subroutines SPHJ and SPHY [10]. After obtaining the scattering phase shifts from different partial waves, the total scattering amplitude $f(k,\theta)$ can be calculated as [8]:

$$f(k,\theta) = \frac{1}{2ik}\sum_{\ell=0}^{\infty}(2\ell+1)P_\ell(\cos\theta)\left[\exp(i2\delta_\ell)-1\right], \tag{10}$$

where $P_\ell(\cos\theta)$ is the Legendre polynomial and $\exp(i2\delta_\ell)$ represent the scattering matrix element. Partial waves from $\ell = 0$ - 120 are considered to ensure the inclusion of all relevant partial waves. The differential cross-section (DCS), which is a measure of the fraction of scattered particles of a given incident momentum in a given direction per unit solid angle, is written by the expression [8]:

$$\frac{d\sigma}{d\Omega} = |f(k,\theta)|^2. \tag{11}$$

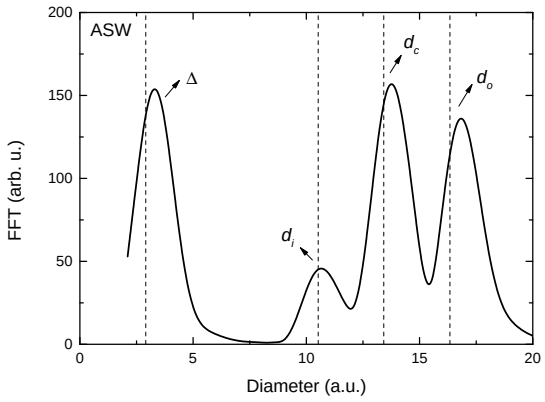

FIG. 2. Fast Fourier transform (FFT) results of DCS computed for ASW potential in partial wave analysis for energy $E = 200$ eV. Vertical lines indicate the C_{60} geometric parameters (see text) that well correspond to FFT peak positions.

BORN APPROXIMATION

To extract the diffraction-encoded structural information using the Fourier transform, we consider the bare ASW potential, Eq. (3), and apply the first-order Born approximation. Thus, the scattering amplitude $f(k,\theta)$ is expressed as:

$$f_{\text{Born}} = \frac{-2m}{\hbar^2}\int_0^\infty V(r)\frac{\sin(qr)}{qr}r^2 dr, \tag{12}$$

where the $q = 2k\sin(\theta/2)$ is the momentum transferred for a given impact energy. When the ASW potential form of $V(r)$ is substituted in Eq. (12) the DCS can be analytically evaluated as:

$$\begin{aligned}\frac{d\sigma}{d\Omega} &= C_1(q) + C_2(q)\cos(2r_i q) + C_3(q)\cos(2r_o q) \\ &+ C_4(q)\cos(2r_c q) + C_5(q)\cos(2\Delta q) + C_6(q)\sin(2r_i q) \\ &+ C_7(q)\sin(2r_o q) + C_8\sin(2r_c q) + C_9(q)\sin(2\Delta q)\end{aligned} \tag{13}$$

where $C_n(q)$'s are coefficients, which are also functions of r_i and r_o. Eq. (13) reveals that the DCS inherently has four oscillation frequencies, which correspond to the geometric features of C_{60}: shell thickness Δ, inner diameter $d_i = 2r_i$, mean diameter $d_c = 2r_c$ and outer diameter $d_o = 2r_o$. In Fig. (2), the fast Fourier transform (FFT) of the numerically obtained DCS data, using Eqs. (10) and (11), is shown. The four distinct peaks confirm that the peak location matches with C_{60}'s geometry.

* jobin.jose@iitp.ac.in
† himadri@nwmissouri.edu

[1] J. Choi, E. Chang, D. M. Anstine, M. E. Madjet, and H. S. Chakraborty, Effects of exchange-correlation potentials on the density-functional description of C_{60} versus C_{240} photoionization, Physical Review A **95**, 023404 (2017).

[2] M. E. Madjet, H. S. Chakraborty, J. M. Rost, and S. T. Manson, Photoionization of C_{60}: a model study, Journal of Physics B: Atomic, Molecular and Optical Physics **41**, 105101 (2008).

[3] V. Dolmatov, M. Cooper, and M. Hunter, Electron elastic scattering off endohedral fullerenes A@C_{60}: The initial insight, Journal of Physics B: Atomic, Molecular and Optical Physics **47**, 115002 (2014).

[4] M. J. Puska and R. M. Nieminen, Photoabsorption of atoms inside C_{60}, Physical Review A **47**, 1181 (1993).

[5] J. De Vries, H. Steger, B. Kamke, C. Menzel, B. Weisser, W. Kamke, and I. Hertel, Single-photon ionization of C_{60}- and C_{70}-fullerene with synchrotron radiation: determination of the ionization potential of C_{60}, Chemical physics letters **188**, 159 (1992).

[6] E. Tosatti and N. Manini, Anomalous attachment of low-energy electrons to C_{60}, Chemical physics letters **223**, 61 (1994).

[7] V. Dolmatov, M. Y. Amusia, and L. Chernysheva, Effects of target polarization in electron elastic scattering off endohedral-A@C_{60}, Physical Review A **95**, 012709 (2017).

[8] C. J. Joachain, *Quantum Collision Theory* (North Holland publishing company, 1975).

[9] J. M. Thijssen, *Computational Physics* (Cambridge university press, 2007).

[10] S. Zhang, J. Jin, and R. E. Crandall, *Computation of Special Functions* (American Association of Physics Teachers, 1997).